Clinical & Experimental Neuroimmunology

Clinical and Experimental Neuroimmunology **4** (2013) 181–192

ORIGINAL ARTICLE

Molecular network of chromatin immunoprecipitation followed by deep sequencing-based (ChIP-Seq) Epstein–Barr virus nuclear antigen 1-target cellular genes supports biological implications of Epstein–Barr virus persistence in multiple sclerosis

Jun-ichi Satoh, Natsuki Kawana and Yoji Yamamoto

Department of Bioinformatics and Molecular Neuropathology, Meiji Pharmaceutical University, Tokyo, Japan

Keywords
chromatin immunoprecipitation followed by deep sequencing;
Epstein–Barr virus; Epstein–Barr virus nuclear antigen 1; GenomeJack; molecular network; multiple sclerosis

Correspondence
Jun-ichi Satoh, MD, Department of Bioinformatics and Molecular Neuropathology, Meiji Pharmaceutical University, 2-522-1 Noshio, Kiyose, Tokyo 204-8588, Japan.
Tel: +81-42-495-8678
Fax: +81-42-495-8678
Email: satoj@my-pharm.ac.jp

Received: 29 March 2013; revised: 17 May 2013; accepted: 24 May 2013.

Abstract

Objectives Epstein–Barr virus (EBV) infection confers a strong risk factor for development of multiple sclerosis (MS). EBV preferentially infects B lymphocytes to establish a life-long latent infection. EBV nuclear antigen 1 (EBNA1), acting as a transcriptional activator, plays a central role in the replication and maintenance of the latent episomal EBV genome in EBV-infected host cells. However, the comprehensive set of host cellular genes directly regulated by EBNA1 relevant to the immunopathogenesis of MS remains to be elucidated.

Methods We investigated the chromatin immunoprecipitation followed by deep sequencing (ChIP-Seq) dataset of Raji cells, an EBV-positive Burkitt's lymphoma cell line. We studied the molecular network of target genes by pathway analysis tools of bioinformatics.

Results We identified the set of 228 EBNA1-target cellular genes. The EBNA1-binding sites were located mainly in intronic regions of target genes with an existence of the palindromic consensus sequence motif. By pathway analysis using Ingenuity Pathways Analysis and KeyMolnet, the EBNA1-target cellular gene network showed a significant relationship with the networks related to cell death and survival, and transcriptional regulation by interferon-regulatory factor (IRF), and signal transducer and activator of transcription (STAT).

Conclusions These results show that the EBNA1-target cellular gene network is closely associated with maintenance of EBV persistence by controlling the fate of EBV-infected host cells, and by aberrantly regulating the production of host-derived antiviral interferons and other cytokines, supporting biological implications of EBV persistence in MS. (Clin. Exp. Neuroimmunol. doi: 10.1111/cen3.12035, July 2013)

Introduction

Epstein–Barr virus (EBV) is a gammaherpesvirus infecting over 90% of the human population, mostly within the first decade of life.[1] By contact with oral secretions, EBV initially infects a subset of nasopharynx epithelial cells to induce replicative and lytic infection, and then the virus preferentially infects B lymphocytes by binding to the CD21 receptor, and immortalizes them to establish a life-long latent infection. The EBV genome consists of a linear DNA that encodes nearly 100 viral proteins essential for the replication and persistence of viral DNA, and modulation of host immune responses. Among nine latency-associated proteins, EBV nuclear antigen 1 (EBNA1) plays a central role in the replication and maintenance of the latent episomal circular EBV genome by binding to the site of the latent origin of replication termed oriP.[2] The oriP site is composed of two distinct loci, such as the family-of-repeats locus (FR) essential for the maintenance of the EBV genome and the dyad symmetry locus (DS) pivotal for

the initiation of replication. In general, EBV-infected cells show distinct patterns of latent gene expression programs termed type I, II or III.[1] EBV is frequently associated with development of certain malignancies, including Burkitt's lymphoma, Hodgkin's disease, nasopharyngeal carcinoma and gastric carcinoma.[3] EBNA1 is the only viral protein consistently expressed throughout all three latency-associated programs, and in all forms of EBV-positive malignancies. Furthermore, EBNA1 serves as a target antigen for both class I major histocompatability complex-restricted CD8+ T cells and class II major histocompatability complex-restricted CD4+ T cells in the host immune system.[4]

EBNA1, through its carboxy-terminal DNA-binding and dimerization domain, forms a stable homodimer that recognizes a specific DNA-binding site located in both viral and host genomes.[5] Increasing evidence shows that EBNA1, by acting as a transcriptional activator, regulates the expression of not only viral proteins essential for latent viral replication, but also a wide range of host cellular genes involved in transcription, translation and cellular signaling.[5–8] EBNA1 increases AP-1 activity by binding directly to the promoters of c-Jun and activating transcription factor 2 (ATF2), resulting in upregulation of interleukin-8, vascular endothelial growth factor, and hypoxia-inducible factor 1α crucial for angiogenesis and metastasis of tumor cells.[9] EBNA1 confers resistance to apoptosis in B lymphoma cells by forming a complex with Sp1 that upregulates the expression of an anti-apoptotic regulator, survivin.[10] Downregulation of EBNA1 by RNA interference inhibits proliferation of Raji cells, an EBV-positive Burkitt's lymphoma cell line.[11] EBNA1 inhibits the canonical nuclear factor-κB pathway in cancer cells by reducing phosphorylation levels of IκB kinase (IKK)α/β.[12]

Accumulating evidence shows that EBV infection confers a strong risk factor for development of MS.[13] MS risk is extremely low in individuals who are negative for EBV, whereas it increases by several fold after EBV infection, assessed by clinical manifestations of infectious mononucleosis, higher serum levels of anti-EBNA complex and anti-EBNA1 antibodies, and increased CD4+ and CD8+ T cell responses against EBV.[14–18] The serum anti-EBNA1 antibody levels increase at 15–20 years before the onset of MS.[19] Periodic reactivation of EBV plays a role in MS relapse, possibly by providing a continuous antigenic stimulation to the immune system.[20] Increased serum anti-EBNA1 immunoglobulin G (IgG) levels predict conversion from clinically isolated syndrome (CIS) to definite MS.[21] Molecular mimicry between EBV antigens and myelin antigens could generate autoreactive T cells.[22] Oligoclonal IgG in the cerebrospinal fluid (CSF) of MS patients reacts with EBNA1.[23] Infiltrating B cells and plasma cells, and ectopic B cell meningeal follicles express EBV latent proteins in MS brains.[24] EBV-infected autoreactive B cells, by acting as antigen presenting cells (APC), enhance EBV-specific T cell immunity.[25] Elevated serum anti-EBV IgG titers correlated with an accumulation of gadolinium-enhancing lesions and progression of grey matter atrophy on magnetic resonance imaging (MRI), and a deterioration of the Expanded Disability Status Scale (EDSS) score in the patients with MS.[26,27] Importantly, clinically effective interferon-β (IFNβ) therapy is associated with a reduction of proliferative T cell responses directed to EBNA1.[28]

At present, the comprehensive set of host cellular genes directly regulated by EBNA1 relevant to the immunopathogenesis of MS remains to be elucidated. Recently, the rapid progress in the next-generation sequencing (NGS) technology has revolutionized the field of genome research. As one of the NGS applications, chromatin immunoprecipitation followed by deep sequencing (ChIP-Seq) provides a highly efficient method for genome-wide profiling of DNA-binding proteins, histone modifications and nucleosomes.[29] ChIP-Seq, which is endowed with an advantage of much higher resolution, less noise and greater coverage of the genome, compared with the microarray-based ChIP-chip method, serves as an innovative tool for studying the comprehensive gene regulatory networks. However, as the NGS analysis produces extremely high-throughput experimental data, it is often difficult to extract the meaningful biological implications. Recent advances in systems biology enable us to illustrate the cell-wide map of the complex molecular interactions by using the literature-based knowledgebase of molecular pathways.[30] The logically arranged molecular networks construct the whole system characterized by robustness, which maintains the proper function of the system in the face of genetic and environmental perturbations. Therefore, the integration of high dimensional NGS data with underlying molecular networks offers a rational approach to characterize the network-based molecular mechanisms of gene regulation on the whole genome scale.

In the present study, to characterize a comprehensive picture of the EBNA1-target cellular gene network relevant to the immunopathogenesis of MS, we investigated the EBNA1 ChIP-Seq dataset of Raji cells retrieved from the public database.

Methods

ChIP-Seq dataset

To identify a comprehensive set of EBNA1-target cellular genes, we investigated ChIP-Seq data retrieved from DDBJ Sequence Read Archive (DRA) (trace.ddbj.nig.ac.jp/DRASearch) under the accession number of SRP015132. In this dataset, ChIP-Seq experiments were carried out by researchers in Dr Paul M. Lieberman's Laboratory.[8] The data were derived from Raji cells, an EBV-positive Burkitt's lymphoma cell line, processed for ChIP with mouse monoclonal anti-EBNA1 antibody (Advanced Biotechnologies, Columbia, MD, USA) or mouse IgG for input control. NGS libraries constructed from 150–300 bp size-selected ChIP DNA fragments were processed for deep sequencing at a 36-bp read length on Genome Analyzer II (Illumina, San Diego, CA, USA).

We converted the dataset of SRALite-formatted files into FASTQ-formatted files. We evaluated the quality of short reads by searching them on the FastQC program (www.bioinformatics.babraham.ac.uk/projects/fastqc). Then, we removed a battery of short reads presenting with insufficient quality by filtering them with the FASTX-toolkit (hannonlab.cshl.edu/fastx_toolkit; Figure S1). After data cleaning, we mapped the short reads on the human genome reference sequence version hg19 by using the Bowtie 0.12.7 program (bowtie-bio.sourceforge.net). Subsequently, we identified statistically significant peaks of mapped reads by using the MACS program (liulab.dfci.harvard.edu/MACS) under the condition that satisfies the false discovery rate (FDR) <5% and fold enrichment (FE) >20 in order to reduce the detection of false positive binding sites if at all possible. Then, we identified the genomic location of MACS peaks by importing the processed data into GenomeJack v1.4, a novel genome viewer for NGS platforms developed by Mitsubishi Space Software (www.mss.co.jp/businessfield/bioinformatics), as described previously.[31]

Based on RefSeq ID, MACS peaks were categorized into the following; the peaks located on protein-coding genes supplemented with NM-heading numbers, the peaks located on non-coding genes supplemented with NR-heading numbers and the peaks located in intergenic regions with no relevant neighboring genes. Genomic locations of the peaks were further classified into the following: the promoter region defined by the location within a 5 kb upstream from the 5′ end of genes, the 5′ untranslated region (5′UTR), the exon, the intron, the 3′ UTR, the location within a 5 kb downstream from the 3′ end of genes (3′down) and intergenic regions outside these, as described previously.[31] The consensus sequence motif was identified by importing a 400 bp-length sequence surrounding the summit of MACS peaks into the MEME-ChIP program (meme.sdsc.edu/meme/cgi-bin/meme-chip.cgi).

Molecular network analysis

To identify biologically relevant molecular networks and pathways, we imported Entrez Gene IDs of EBNA1-target cellular genes into the Functional Annotation tool of Database for Annotation, Visualization and Integrated Discovery (DAVID) v6.7 (david.abcc.ncifcrf.gov).[32] We also imported them into Ingenuity Pathways Analysis (IPA; Ingenuity Systems; www.ingenuity.com) and KeyMolnet (Institute of Medicinal Molecular Design; www.immd.co.jp), both of which are commercial bioinformatics tools for analyzing molecular interactions on the comprehensive knowledgebase.

IPA is a knowledgebase that contains approximately 3000000 biological and chemical interactions, and functional annotations with definite scientific evidence. By uploading the list of Gene IDs and expression values, the network-generation algorithm identifies focused genes integrated in a global molecular network. IPA calculates the score *P*-value that reflects the statistical significance of association between the genes and the networks by the Fisher's exact test.

KeyMolnet contains knowledge-based contents on 157700 relationships among human genes and proteins, small molecules, diseases, pathways, and drugs.[30] They are categorized into the core contents collected from selected review articles with the highest reliability or the secondary contents extracted from abstracts on PubMed and the Human Reference Protein database. By importing the list of Gene ID and expression values, KeyMolnet automatically provides corresponding molecules as nodes on the network. Among various network-searching algorithms, the "N-points to N-points" search extracts the molecular network with the shortest route connecting the starting point molecules and the end-point molecules. The generated network was compared side by side with 492 human canonical pathways of the KeyMolnet library. The library contains a selected set of 92 MS-linked molecules closely related to the immunopathogenesis of MS, curated by expert biologists (Table S1). The algorithm counting the number of overlapping molecular relations between the extracted network and the

canonical pathway makes it possible to identify the canonical pathway showing the most significant contribution to the extracted network.[30]

Results

Identification of 228 ChIP-Seq-based EBNA1-target cellular genes

After mapping short reads on hg19, we identified a total of 418 ChIP-Seq peaks that satisfied the criteria of both FDR <5% and FE >20. Then, the genomic location of the peaks was determined by GenomeJack. After omitting the peaks located in non-coding genes, those located in intergenic regions and several redundant genes, we finally extracted 228 peaks located in protein-coding genes (top 20 shown in Table 1; the complete list shown in Table S2). They are tentatively designated as the whole set of ChIP-Seq-based EBNA1-target cellular genes. Among 228 genes, the set of 45 genes (19.7%) were reported as the genes having EBNA1-binding sites by previous ChIP-chip or ChIP-Seq studies[6–8] (Table S2). They include *UBALD2* (alternatively named *FAM100B*; Fig. 1), *PIPK5K1B*, *FAM122A*, *LAIR1*, *CLIC1*, *CCDC6*, *RRAS*, *SCAF1*, *SYNE2*, *NEK6*, *SPAG1*, *GPR110*, *FOXP2*, *IL6R* (Fig. 2), *MDM1*, *RNF169*, *DEK*, *CDC7* (Fig. 3), *INSL6*, *PRKR1A*, *POU2F1*, *DGKB*, *CYB5A*, *RNF145*, *KRIT1*, *ANKIB1*, *BEGAIN*, *CORO1A*, *RCC1*, *ITPKB*, *PARK2*, *ACE*, *KDM4C*, *SIVA1*, *TAB 2*, *ADSSL1*, *PPP1R16B*, *HPX*, *TRIM3*, *ABCC12*, *GLIS3*, *NFE2L3*, *AMCAR*, *SNED1* and *BCL6*. The summits of the peaks were located in the promoter (n = 34; 14.9%), 5′ UTR (n = 1; 0.4%), exon (n = 5; 2.2%), intron (n = 161; 70.6%), 3′UTR (n = 4; 1.8%), or 3′down (n = 23; 10.1%).

By motif analysis of the top 100 EBNA1-binding regions based on FE with MEME-ChIP, the most significant consensus sequence represented a palindromic motif defined as 5′ [G/A]GG[T/C]AG[C/T/G]A[T/A][G/A]TGCT[G/A]CCC[A/G]3′ (E-value = 3.4e-339; Fig. 4), being consistent with the motifs reported by previous studies,[7,8] supporting the validity of the set of ChIP-Seq-based EBNA1-target cellular genes we identified.

Molecular network of ChIP-Seq-based EBNA1-target cellular genes

Next, we studied the molecular network of 228 ChIP-Seq-based EBNA1-target cellular genes by

Table 1 Top20 ChIP-Seq-based EBNA1-target cellular genes

Chromosome	Start	End	FE	FDR	Entrez Gene ID	Gene Symbol	Location	Gene name
chr17	74258997	74259859	133.47	0	283991	UBALD2	Promoter	UBA-like domain containing 2
chr10	71394130	71395064	92.16	4.17	8395	PIPK5K1B	Intron	Phosphatidylinositol-4-phosphate 5-kinase, type I, beta
chr9	71394130	71395064	92.16	4.17	116224	FAM122A	Promoter	Family with sequence similarity 122A
chr1	53461960	53463107	83.65	3.33	6342	SCP2	Intron	Sterol carrier protein 2
chr19	2800219	2801292	83.24	4	7064	THOP1	Intron	Thimet oligopeptidase 1
chr19	54875945	54877064	82.01	2.7	3903	LAIR1	5′UTR	Leukocyte-associated immunoglobulin-like receptor 1
chr6	31702439	31703232	79.49	3.85	1192	CLIC1	Intron	Chloride intracellular channel 1
chr18	64215734	64216785	75.4	1.82	28513	CDH19	Intron	Cadherin 19, type 2
chr1	24281505	24282331	74.63	4.35	55629	PNRC2	Promoter	Proline-rich nuclear receptor coactivator 2
chr13	100289097	100290016	73.81	2.44	171425	CLYBL	Intron	Citrate lyase beta like
chr16	65953211	65953691	73.73	2.56	9187	SLC24A1	3′down	Solute carrier family 24 (sodium/potassium/calcium exchanger), member 1
chr15	65953211	65953691	73.73	2.56	10260	DENND4A	3′UTR	DENN/MADD domain containing 4A
chr17	63151565	63152489	70.38	2.22	8787	RGS9	Intron	Regulator of G-protein signaling 9
chr10	61668622	61669369	68.89	2	8030	CCDC6	Promoter	Coiled-coil domain containing 6
chr20	50146683	50147387	67.03	1.92	6237	RRAS	Promoter	Related RAS viral (r-ras) oncogene homolog
chr10	38313577	38314346	67.03	1.79	7581	ZNF33A	Intron	Zinc finger protein 33A
chr19	50146683	50147387	67.03	1.92	58506	SCAF1	Intron	SR-related CTD-associated factor 1
chr17	32235096	32235916	65.35	1.89	40	ACCN1	Intron	Amiloride-sensitive cation channel 1, neuronal
chr14	64535928	64536882	62	2.9	23224	SYNE2	Intron	Spectrin repeat containing, nuclear envelope 2
chr18	12256595	12257238	58.65	2.67	1149	CIDEA	Intron	Cell death-inducing DFFA-like effector a

By analyzing the EBNA1 ChIP-Seq dataset numbered SRP015132, we identified 228 MACS peaks on protein-coding genes that satisfy the criteria of both false discovery rate (FDR) smaller than 5% and fold enrichment (FE) greater than 20. Top 20 genes based on FE are listed with the chromosome, the position (start, end), FE, FDR, Entrez Gene ID, Gene Symbol, the location (promoter, 5′UTR, exon, intron, 3′UTR, 3′down), and Gene Name.

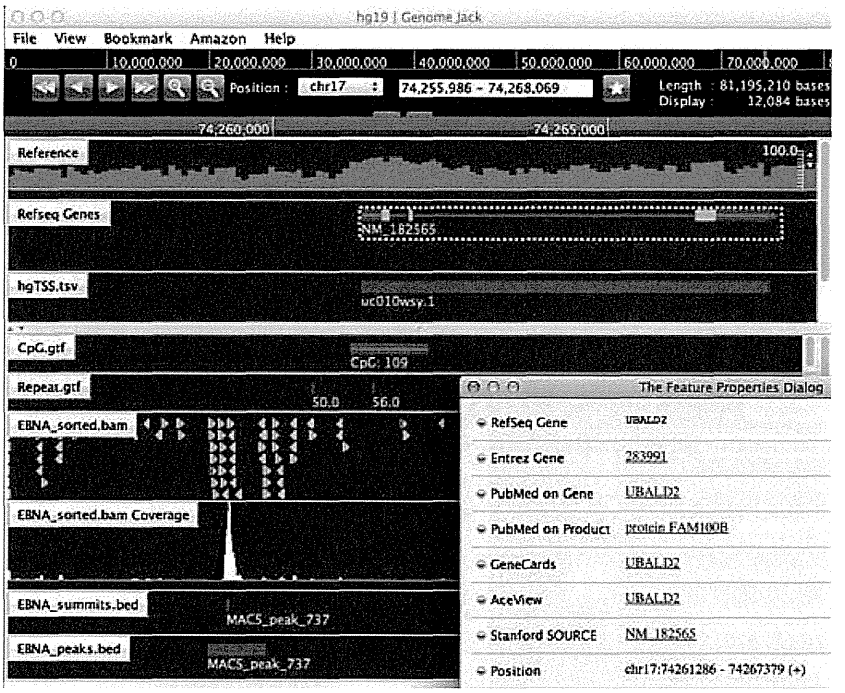

Figure 1 The genomic location of an Epstein–Barr virus nuclear antigen 1 (EBNA1) chromatin immunoprecipitation followed by deep sequencing (ChIP-Seq) peak in the promoter region of UBALD2. By analyzing the dataset numbered SRP015132, we identified a total of 228 EBNA1 ChIP-Seq peaks that satisfied the criteria of both false discovery rate <5% and fold enrichment) >20. The genomic location of the peaks was determined by importing the processed data into GenomeJack. An example of UBA-like domain containing 2 (*UBALD2*, alternatively named *FAM100B*; Entrez Gene ID 283991, composed of a single transcript NM_182565, is shown, where a MACS peak numbered 737 is located in the promoter region of *UBALD2*.

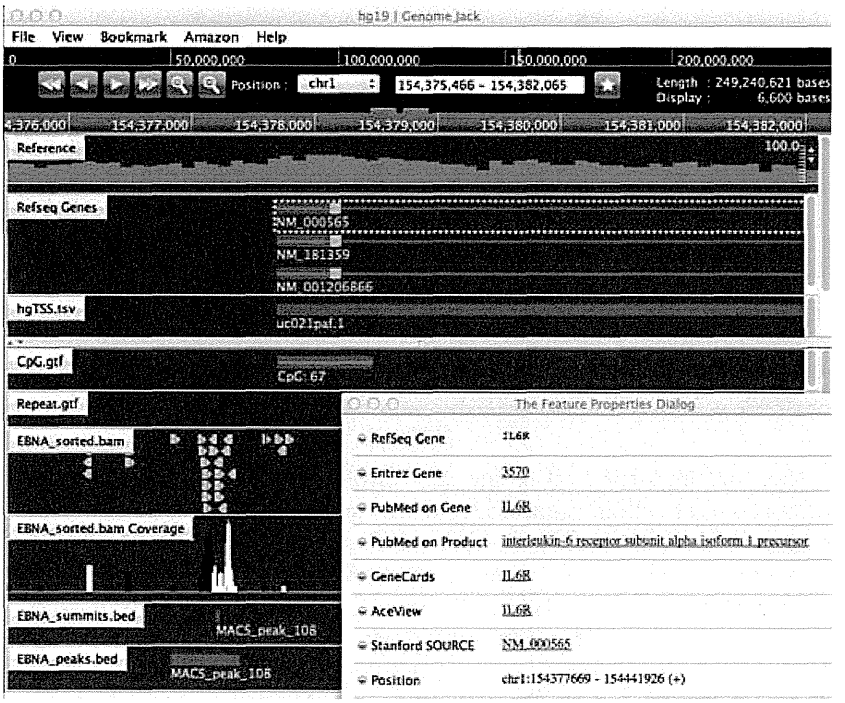

Figure 2 The genomic location of an Epstein–Barr virus nuclear antigen 1 (EBNA1) chromatin immunoprecipitation followed by deep sequencing (ChIP-Seq) peak in the promoter region of *IL6R*. The genomic location of EBNA1 ChIP-Seq peaks was determined by GenomeJack. An example of interleukin-6 receptor (IL-6R; Entrez Gene ID 3570), composed of three transcript variants NM_000565, NM_181359 and NM_001206866, is shown, where a MACS peak numbered 108 is located in the promoter region of *IL6R*.

using bioinformatics tools for analyzing molecular interactions on the comprehensive knowledgebase. First, DAVID identified statistically significant functionally associated gene ontology (GO) terms. They included "regulation of cell motion" (GO:0051270; $P = 0.000006$), "plasma membrane part" (GO:0044459; $P = 0.000039$) and "apical plasma membrane" (GO:0016324; $P = 0.000116$), as the top three most significant GO terms. These results suggest that ChIP-Seq-based EBNA1-target cellular genes play a key role in maintenance of plasma membrane integrity.

Figure 3 The genomic location of an Epstein–Barr virus nuclear antigen 1 (EBNA1) chromatin immunoprecipitation followed by deep sequencing (ChIP-Seq) peak in the promoter region of CDC7. The genomic location of EBNA1 ChIP-Seq peaks was determined by GenomeJack. An example of cell division cycle 7 homolog (CDC7; Entrez Gene ID 8317), composed of three transcript variants NM_003503, NM_001134419 and NM_001134420, is shown, where a MACS peak numbered 94 is located in the promoter region of CDC7.

Figure 4 *Identification of an Epstein–Barr virus nuclear antigen 1 (EBNA1)-binding consensus sequence motif. The consensus sequence motif was* identified by importing a 400 bp-length sequence surrounding the summit of MACS peaks of the top 100 EBNA1-binding regions based on fold enrichment (FE) into the MEME-ChIP program, which identified the most significant motif defined as 5′[G/A]GG[T/C]AG[C/T/G]A[T/A][G/A]TGCT[G/A]CCC[A/G]3′.

Next, by importing all of the 228 ChIP-Seq-based EBNA1-target cellular genes, IPA at the setting of 70 molecules/net extracted the networks defined by "Nutritional Disease, Cell Death and Survival, Cellular Development" (P = 1.00E-67; Fig. 5), "Developmental Disorder, Hereditary Disorder, Cellular Movement" (P = 1.00E-51) and "Cellular Assembly and Organization, Cellular Function and Maintenance, Cell-To-Cell Signaling and Interaction" (P = 1.00E-47), as the top three most significant functional networks (Table 2). By importing the set of 34 ChIP-Seq-based EBNA1-target cellular genes that had the peak location in promoter regions, IPA at the setting of 35 molecules/net extracted the networks defined by "Cell Morphology, Cellular Compromise, Cellular Assembly and Organization" (P = 1.00E-36) and "Cancer, Cell Death and Survival, Cellular Development" (P = 1.00E-33) as the most relevant functional networks, supporting the reproducibility of the molecular network analysis. These results suggest that ChIP-Seq-based EBNA1-target cellular genes play a central role in regulation of cell death and survival, development, and other various cellular functions.

Finally, KeyMolnet, by using the "N-points to N-points" search starting from 228 genes and ending at 92 MS-linked molecules (Table 1), extracted the highly complex molecular network composed of 1569 molecules and 4450 molecular relations. This network showed the most significant relationship

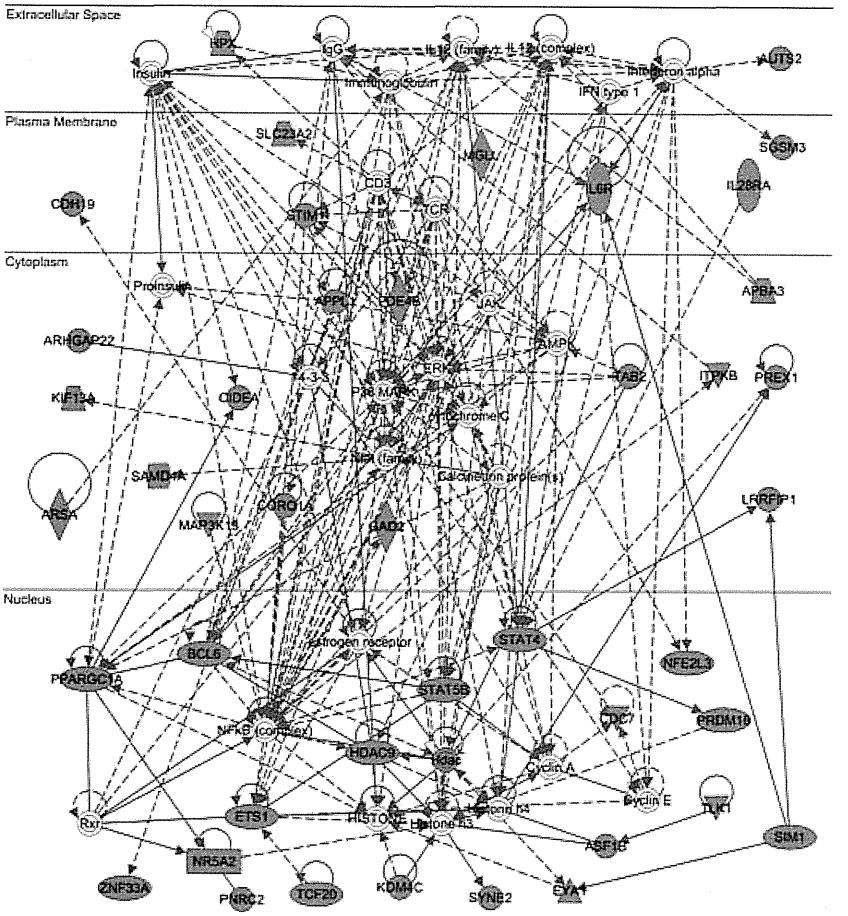

Figure 5 Ingenuity Pathways Analysis (IPA) functional networks of chromatin immunoprecipitation followed by deep sequencing (ChIP-Seq)-based Epstein–Barr virus nuclear antigen 1 (EBNA1)-target cellular genes. Entrez Gene IDs of 228 ChIP-Seq-based EBNA1-target cellular genes were imported into the core analysis tool of IPA. It extracted functional networks relevant to the set of imported genes under the condition of 70 molecules per network (Table 2). The first rank network termed "Nutritional Disease, Cell Death and Survival, Cellular Development" is shown, where *EBNA1*-target cellular genes are colored by red.

with canonical pathways defined by "transcriptional regulation by interferon-regulatory factor (IRF)" (P = 1.97E-80), "mitogen-activated protein kinase (MAPK) signaling pathway" (P = 1.58E-79), "transcriptional regulation by mothers against decapentaplegic homolog (SMAD)" (P = 5.05E-77), "transcriptional regulation by signal transducer and activator of transcription (STAT)" (P = 1.51E-68), "transcriptional regulation by retinoid X receptor (RXR)" (P = 6.45E-67) and "transcriptional regulation by p53" (P = 6.57E-62; Fig. 6). These results suggest that ChIP-Seq-based EBNA1-target cellular genes are closely related to various cellular signaling pathways involved in production of host-derived interferons and other cytokines in response to latent EBV infection.

Discussion

In the present study, we identified the comprehensive set of 228 EBNA1-target cellular genes derived from the ChIP-Seq dataset of Raji cells, an EBV-infected Burkitt's lymphoma cell line. The EBNA1-binding sites were located mainly in intronic regions (70.6%) of target genes with an existence of the palindromic consensus sequence motif. However, it is not surprising, because a recent study showed that the binding sites of EBNA2 to the host cellular genome, another protein associated with EBV latency, are located predominantly in intronic and intergenic regions, but rarely in promoter regions.[33] Among 228 EBNA1-target cellular genes, the set of 45 genes (19.7%), including *UBALD2* (*FAM100B*), *IL6R* and *CDC7*, have met with the genes previously identified by ChIP-chip or ChIP-Seq studies,[6–8] supporting the validity of our observations. It is worthy to note that EBV promotes *IL6R* expression in immortalized B cells and Burkitt's lymphoma cells.[34]

The ChIP-Seq technology has an advantage of higher resolution, less noise and greater coverage of the genome, compared with the microarray-based ChIP-chip method.[29] Although ChIP-Seq serves as a highly efficient method for genome-wide profiling of DNA-binding proteins, the method intrinsically requires several technical considerations.[35] The specificity of the antibody, reproducibility of the results,

Table 2 IPA functional networks relevant to 228 ChIP-Seq-based EBNA1-target cellular genes

Rank	Category	Molecules in network	*P*-value
1	Nutritional disease, cell death and survival, cellular development	14-3-3, AMPK, APBA3, APPL1, ARHGAP22, ARSA, ASF1B, AUTS2, BCL6, Calcineurin protein(s), CD3, CDC7, CDH19, CIDEA, CORO1A, Cyclin A, Cyclin E, cytochrome C, ERK, estrogen receptor, ETS1, EYA1, GAD2, HDAC9, Hdac, HISTONE, Histone h3, Histone h4, HPX, IFN type 1, IgG, IL12 (complex), IL12 (family), IL28RA, IL6R, Immunoglobulin, Insulin, Interferon alpha, ITPKB, JAK, KDM4C, KIF13A, LRRFIP1, MAP3K13, MGLL, Nfat (family), NFE2L3, NFkB (complex), NR5A2, P38 MAPK, PDE4B, PNRC2, PPARGC1A, PRDM16, PREX1, Proinsulin, Rxr, SAMD4A, SGSM3, SIM1, SLC23A2, STAT4, STAT5B, STIM1, SYNE2, TAB2, TCF20, TCR, TLK1, ZNF33A	1.00E-67
2	Developmental disorder, hereditary disorder, cellular movement	ACE, ADAM12, Alp, AMACR, Ap1, CACNA1D, CAMK2A, CaMKII, CCDC6, Cofilin, COL5A1, Collagen Alpha1, Collagen type I, Collagen type II, Collagen type IV, Collagen(s), creatine kinase, Creb, EGFR, ERK1/2, Focal adhesion kinase, GHR, GIT1, growth factor receptor, Growth hormone, HIVEP3, HSPG2, IARS, IGF1R, IL1, INSL6, Integrin, ITGA11, KCNMA1, LAIR1, Laminin, LDL, Mek, mGluR, MYLK, NCK, NF1, NMDA Receptor, NRG1, OVGP1, p70 S6k, PAK3, Pak, Pdgf (complex), PDGF BB, PLC gamma, PP1 protein complex group, PP2A, Ppp2c, Rap1, RRAS, SHB, SORL1, Sos, SOX6, SPARC, STAT5a/b, Tgf beta, TGFBI, TSH, UNC5C, Wnt, WNT5A, WNT5B, WNT9B	1.00E-51
3	Cellular assembly and organization, cellular function and maintenance, cell-to-cell signaling and interaction	26s Proteasome, ABCC2, Actin, ADAM11, ADCY, Akt, Alpha catenin, ANXA6, ATG7, Calmodulin, calpain, caspase, Cg, CLIC1, Dgk, DGKB, DGKD, F Actin, FSH,G protein, G protein alpha, G protein beta gamma, G-protein beta, GNA14, GNAQ, GNRH, Gpcr, GPR110, GRM4, GRM8, HCRTR1, IQSEC1, Jnk, Lh, Mapk, Metalloprotease, MFN1, MKL1, NPY, OPCML, OSTF1, p85 (pik3r), PARD3, PARK2, PCNX, PDE2A, PI3K (complex), PIP5K1B, Pka, Pkc(s), PLC, PLXNA2, PLXNB2, POU2F1, PRKAR1A, Rac, Ras, Ras homolog, RCC1, RNA polymerase II, SIVA1, STARD13, STAT, SYN2, SYNM, THOP1, trypsin, VANGL2, Vegf, XPO6	1.00E-47
4	Developmental disorder, hematological disease, hereditary disorder	ANKIB1, ANO6, ATP6, BCDIN3D, BEGAIN, BRWD1, BTBD9, C17orf28, CHCHD6, CLIP3, CSMD3, DAZ1/DAZ4, DNAJC11, DZIP3, EML2, EML3, EML4, FAM122A, GOLPH3, GPR37, GPR179, GPRC5A, GPRC5C, HLCS, IFT43, IPMK, KCTD5, KIAA0284, LGR4, LGR5, LPHN1, LRRC41, MAP1LC3A, MAPK1IP1L, MTX1, MTX2, MYO18A, MYO18B, NCAPG2, NCKAP5L, NEK6, NEK7, NEURL4, PCCA, PCCB, PCID2, PCNX, PPP2R2B, QSOX1, RHOBTB3, RNF38, RNF145, RNF169, RNF187, RSPO2, SAMM50, SCAF1, SPAG1, SURF4, TBC1D2, TRMT1, TULP3, UBA6, UBC, UBE2R2, UBR3, UCK2, VWA5A, ZG16B, ZRANB3	1.00E-47
5	Cell signaling, organ morphology, organismal development	ADSSL1, BCAS1, beta-estradiol, Betacatenin/TCF, CLYBL, CNN2, COA1, COX17, COX6A2, CST4, CTNNB1, CXXC4, CYB5A, DEK, DLG2, DUSP7, DUSP12, EML2, EVX1, FAT3, FGF1, FGF18, FGFBP1, FRMD3, GPATCH4, GPR179, GPRC5A, GPRC6A, GTF2A1, HCRTR1, HDL-cholesterol, HNF1A, IL17RD, INSL6, KISS1R, LMX1B, LYL1, MAPK1, MPZL2, MYBL1, NMBR, NOL8, NPAS4, NPFFR2, PAMR1, PCCA, PCDH9, PDZK1IP1, PGLYRP1, PRLHR, PTPRD, RGS9, RYK, SCP2, SGMS1, SHANK2, SHC4, SIX6, SMPDL3A, SNED1, SPAG16, SSTR4, SUMO2, TMEM87A, TRANK1, USO1, VAX2, WNT5B, YWHAZ, ZNF217	1.00E-42
6	Cellular development, hematological system development and function, hematopoiesis	ABCC12, ANKRD6, ANKS1A, ARAP2, ATP2A3, ATP5D, ATP6V1B1, CD48, CLASP1, CLPX, CMIP, COX6A2, CTU1, DENND4A, DNAJC4, DNAJC11, DNM3, Endophilin, FAS, FGFR2, FNBP4, FOXE1, FYN, GLIS3, GPT2, GSK3B, H2BFM, HSPA4, HTT, IFNG, IL20RB, IL22RA1, INS, iron, KIAA0101, KIF1B, KRIT1, KRT37, LUC7L, MACF1, MAFA, MC3R, MDH2, MRPL54, MYL4, NDUFB4, PAX4, PGLYRP1, PPP1R16B, PRKCDBP, PTPN22, RHAG, RHCE/RHD, RRAGD, SCAMP5, SEPP1, SETBP1, SLC24A1, SMARCA4, SRRT, SRSF4, SRSF6, TCF3, TGFBI, TRIM3, YWHAG, ZMYND8, ZNF277, ZNF33B, ZP3	1.00E-33
7	Cell morphology, cellular function and maintenance, reproductive system development and function	AGT, AK4, ALKBH6, ANKRD28, ANKRD44, ANKRD52, ANKS4B, APH1A, APP, AQP8, ARPC5, ASIC2, ASIC3, ATXN7L1, C12orf49, C2orf44, C6orf170, C9orf72, CDK4, CFL2, CLIC1, CLPX, CYP3A43, DDAH1, DSC2, DSCAML1, EDEM1, ELAVL1, FAM117B, FDX1, FOXP2, GALM, GBE1, GFM1, GLCE, GPC6, GPM6B, HNF4A, HSPG2, IL1A, INHBA, ITIH3, KIF2C, LONP2, MAPRE2, MFSD1, MTMR2, MYCL1, NDFIP2, NEK7, NFIX, NMNAT2, ODZ4, PAK3, PCDH9, PDZK1IP1, PIR, PLK1, PPP6R2, PTBP2, RPL41, SLC13A1, SLC38A4, SMCR8, SPON1, SRPR, STOML1, WDR41, ZNF423, ZNHIT6	1.00E-28

By importing Entrez Gene IDs of 228 ChIP-Seq-based EBNA1-target cellular genes into the core analysis tool of IPA, functional networks showing significant relevance to the imported genes were identified. They are listed with the category of functional networks, focused molecules, and *P*-value by the Fisher's exact test. The first rank network is illustrated in Fig. 5.

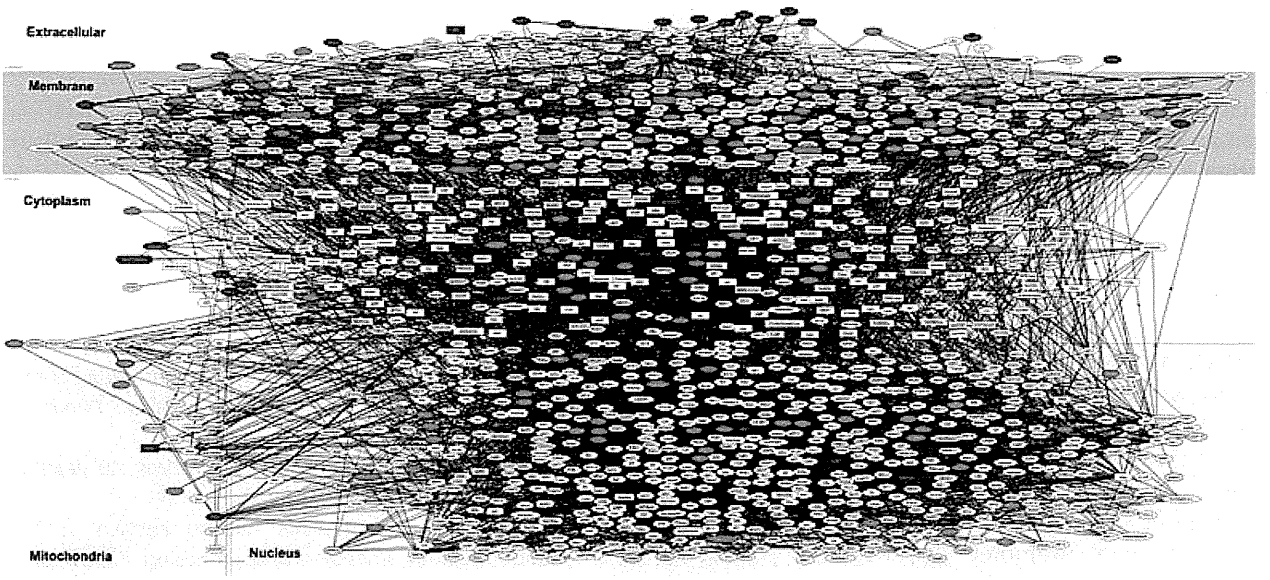

Figure 6 KeyMolnet networks of chromatin immunoprecipitation followed by deep sequencing (ChIP-Seq)-based Epstein–Barr virus nuclear antigen 1 (EBNA1)-target cellular genes. Entrez Gene IDs of 228 ChIP-Seq-based EBNA1-target cellular genes were imported into KeyMolnet. The "N-points to N-points" search starting from 228 genes and ending at 92 MS-linked molecules extracted the highly complex molecular network composed of 1569 molecules and 4450 molecular relations. Red nodes represent *EBNA1*-target cellular genes, whereas blue nodes indicate multiple sclerosis (MS)-linked molecules of the KeyMolnet library. White nodes exhibit additional nodes extracted automatically from the core contents of KeyMolnet to establish molecular connections. The molecular relation is shown by a solid line with an arrow (direct binding or activation), solid line with an arrow and stop (direct inactivation), solid line without an arrow (complex formation), dash line with an arrow (transcriptional activation) and dash line with an arrow and stop (transcriptional repression).

sequencing depth and the source of controls, along with cell types, developmental stages and culture conditions capable of affecting epigenetic features, constitute critical factors. In general, DNA-binding by transcription factors that recruit the complex of auxiliary factors, including coactivators and corepressors, is a highly dynamic process. The ChIP-Seq data reflect a snapshot of binding actions of limited DNA-binding factors onto responsive elements, not always corresponding to their biological activities. However, motif analysis of a defined set of high-quality peaks makes it possible to evaluate the antibody specificity, and to predict the specificity of DNA-protein interaction to some extent.[35]

EBNA1 regulates the expression of various host cellular genes involved in transcription, translation and signaling pathways.[5–8] By ChIP-chip analysis of an EBV-positive lymphoblastoid cell line named 721, a previous study identified 247 promoter regions as candidates for EBNA1-binding sites.[7] They identified the sequence defined by GRTAGCNNNNGCTAYC, where R is purine and Y is pyrimidine, as a degenerate consensus EBNA1-binding motif. Importantly, EBNA1 binding to the promoters of some target genes does not always activate their expression, when assessed by reporter assays.[7] EBNA1 also plays a pivotal role in global remodeling of chromation architecture, thereby affecting the transcription of a wide range of cellular genes through an epigenetic mechanism.[36] By ChIP-chip analysis of a human B cell line named BJAB and HEK293 cells following introduction of an exogenous EBNA1 gene, a different study identified 45 promoter regions of host cellular genes as candidates for EBNA1-binding sites.[6] They showed that EBNA1-target cellular genes are variable among distinct cell types. By using gene expression microarray, they identified 37 promoter sites for upregulated genes and 39 promoter sites for downregulated genes following stable expression of EBNA1, both of which showed distinct consensus binding-site sequences.[6] By ChIP-Seq analysis of Raji cells, a more recent study identified a number of EBNA1-binding sites, detected based on less stringent criteria compared with the present study, although they did not characterize a global picture of the EBNA1-target cellular gene network with relevance to the immunopathogenesis of MS.[8] They found that EBNA1-binding motifs are fairly different between the host cellular target genes and those of the viral genome, suggesting the possibility that certain cellular EBNA1-binding sites reflect an indirect binding site.[8]

By using bioinformatics tools for analyzing molecular interactions on the comprehensive knowledge-base, here we showed that the EBNA1-target cellular gene network is closely associated with regulation of cell death and survival, development and other various cellular functions. These observations suggest that the EBNA1-target cellular gene network plays a key role in maintenance of EBV persistence by controlling the fate of EBV-infected host cells. The network is also associated with molecular networks defined by transcriptional regulation by IRF, SMAD, STAT, RXR, and p53, suggesting that it plays a regulatory role in production of host-derived antiviral interferons and other cytokines. Importantly, EBNA1 enhances the expression of STAT1 that further sensitizes the cells to interferon-induced STAT1 activation.[37] In turn, the JAK-STAT pathway activates the viral promoter, Qp, which is pivotal for transcription of the *EBNA1* gene in the type I latency program.[38] In contrast, BZLF1, an immediate-early protein of EBV, inhibits the expression of IRF3 and IRF7, leading to decreased expression of the host-derived IFNβ.[39] The EBV LF2 tegument protein also acts as an antagonist for type I interferon signaling by interfering with IRF7 dimerization, providing a mechanism responsible for viral evasion of the host-derived IFN-mediated antiviral immune response.[40] Furthermore, EBNA1 suppresses transforming growth factor-β signaling by decreasing the half-life of Smad2, leading to deficient expression of tumor suppressor protein, PTPRK, which is responsible for permanent proliferation of EBV-infected cells.[41] Importantly, MDM2-dependent degradation of p53 is pivotal for B cell transformation by EBV, and the survival of infected cells.[42] All of these observations support the view that EBNA1 plays a key role in viral persistence and evasion of antiviral immune responses in EBV-infected B cells.

In conclusion, we identified the comprehensive set of 228 EBNA1-target cellular genes derived from the ChIP-Seq dataset of Raji cells. Pathway analysis showed that the EBNA1-target cellular gene network is closely associated with maintenance of EBV persistence by controlling the fate of EBV-infected host cells, and by aberrantly regulating the production of host-derived antiviral interferons and other cytokines, supporting biological implications of EBV persistence in MS.

Acknowledgements

This work was supported by grants from the Research on Intractable Diseases (H21-Nanchi-Ippan-201; H22-Nanchi-Ippan-136), the Ministry of Health, Labour and Welfare (MHLW), Japan, and the High-Tech Research Center (HRC) Project (S0801043), and the JSPS KAKENHI (C22500322, C25430054), the Ministry of Education, Culture, Sports, Science and Technology (MEXT), Japan.

References

1. Cohen JI. Epstein-Barr virus infection. *N Engl J Med.* 2000; **343**: 481–92.
2. Hammerschmidt W, Sugden B. Epstein-Barr virus sustains Burkitt's lymphomas and Hodgkin's disease. *Trends Mol Med.* 2004; **10**: 331–6.
3. Young LS, Rickinson AB. Epstein-Barr virus: 40 years on. *Nat Rev Cancer.* 2004; **4**: 757–68.
4. Münz C. Epstein-barr virus nuclear antigen 1: from immunologically invisible to a promising T cell target. *J Exp Med.* 2004; **199**: 1301–4.
5. Westhoff Smith D, Sugden B. Potential cellular functions of Epstein-Barr nuclear antigen 1 (EBNA1) of Epstein-Barr virus. *Viruses.* 2013; **5**: 226–40.
6. Canaan A, Haviv I, Urban AE, Schulz VP, Hartman S, Zhang Z, et al. EBNA1 regulates cellular gene expression by binding cellular promoters. *Proc Natl Acad Sci USA.* 2009; **106**: 22421–6.
7. Dresang LR, Vereide DT, Sugden B. Identifying sites bound by Epstein-Barr virus nuclear antigen 1 (EBNA1) in the human genome: defining a position-weighted matrix to predict sites bound by EBNA1 in viral genomes. *J Virol.* 2009; **83**: 2930–40.
8. Lu F, Wikramasinghe P, Norseen J, Tsai K, Wang P, Showe L, et al. Genome-wide analysis of host-chromosome binding sites for Epstein-Barr virus nuclear antigen 1 (EBNA1). *Virol J.* 2010; **7**: 262.
9. O'Neil JD, Owen TJ, Wood VH, Date KL, Valentine R, Chukwuma MB, et al. Epstein-Barr virus-encoded EBNA1 modulates the AP-1 transcription factor pathway in nasopharyngeal carcinoma cells and enhances angiogenesis *in vitro*. *J Gen Virol.* 2008; **89**: 2833–42.
10. Lu J, Murakami M, Verma SC, Cai Q, Haldar S, Kaul R, et al. Epstein-Barr Virus nuclear antigen 1 (EBNA1) confers resistance to apoptosis in EBV-positive B-lymphoma cells through up-regulation of survivin. *Virology.* 2011; **410**: 64–75.
11. Hong M, Murai Y, Kutsuna T, Takahashi H, Nomoto K, Cheng CM, et al. Suppression of Epstein-Barr nuclear antigen 1 (EBNA1) by RNA interference inhibits proliferation of EBV-positive Burkitt's lymphoma cells. *J Cancer Res Clin Oncol.* 2006; **132**: 1–8.
12. Valentine R, Dawson CW, Hu C, Shah KM, Owen TJ, Date KL, et al. Epstein-Barr virus-encoded EBNA1 inhibits the canonical NF-kB pathway in carcinoma cells by inhibiting IKK phosphorylation. *Mol Cancer.* 2010; **9**: 1.

13. Ascherio A, Munger KL. Epstein-Barr virus infection and multiple sclerosis: a review. *J Neuroimmune Pharmacol.* 2010; **5**: 271–7.
14. Thacker EL, Mirzaei F, Ascherio A. Infectious mononucleosis and risk for multiple sclerosis: a meta-analysis. *Ann Neurol.* 2006; **59**: 499–503.
15. Levin LI, Munger KL, O'Reilly EJ, Falk KI, Ascherio A. Primary infection with the Epstein-Barr virus and risk of multiple sclerosis. *Ann Neurol.* 2010; **67**: 824–30.
16. Munger KL, Levin LI, O'Reilly EJ, Falk KI, Ascherio A. Anti-Epstein-Barr virus antibodies as serological markers of multiple sclerosis: a prospective study among United States military personnel. *Mult Scler.* 2011; **17**: 1185–93.
17. Lünemann JD, Edwards N, Muraro PA, Hayashi S, Cohen JI, Münz C, et al. Increased frequency and broadened specificity of latent EBV nuclear antigen-1-specific T cells in multiple sclerosis. *Brain.* 2006; **129**: 1493–506.
18. Jilek S, Schluep M, Meylan P, Vingerhoets F, Guignard L, Monney A, et al. Strong EBV-specific CD8+ T-cell response in patients with early multiple sclerosis. *Brain.* 2008; **131**: 1712–21.
19. DeLorenze GN, Munger KL, Lennette ET, Orentreich N, Vogelman JH, Ascherio A. Epstein-Barr virus and multiple sclerosis: evidence of association from a prospective study with long-term follow-up. *Arch Neurol.* 2006; **63**: 839–44.
20. Wandinger K, Jabs W, Siekhaus A, Bubel S, Trillenberg P, Wagner H, et al. Association between clinical disease activity and Epstein-Barr virus reactivation in MS. *Neurology.* 2000; **55**: 178–84.
21. Lünemann JD, Tintoré M, Messmer B, Strowig T, Rovira A, Perkal H, et al. Elevated Epstein-Barr virus-encoded nuclear antigen-1 immune responses predict conversion to multiple sclerosis. *Ann Neurol.* 2010; **67**: 159–69.
22. Lang HL, Jacobsen H, Ikemizu S, Andersson C, Harlos K, Madsen L, et al. A functional and structural basis for TCR cross-reactivity in multiple sclerosis. *Nat Immunol.* 2002; **3**: 940–3.
23. Cepok S, Zhou D, Srivastava R, Nessler S, Stei S, Büssow K, et al. Identification of Epstein-Barr virus proteins as putative targets of the immune response in multiple sclerosis. *J Clin Invest.* 2005; **115**: 1352–60.
24. Serafini B, Rosicarelli B, Franciotta D, Magliozzi R, Reynolds R, Cinque P, et al. Dysregulated Epstein-Barr virus infection in the multiple sclerosis brain. *J Exp Med.* 2007; **204**: 2899–912.
25. Pender MP. Infection of autoreactive B lymphocytes with EBV, causing chronic autoimmune diseases. *Trends Immunol.* 2003; **24**: 584–8.
26. Farrell RA, Antony D, Wall GR, Clark DA, Fisniku L, Swanton J, et al. Humoral immune response to EBV in multiple sclerosis is associated with disease activity on MRI. *Neurology.* 2009; **73**: 32–8.
27. Zivadinov R, Zorzon M, Weinstock-Guttman B, Serafin M, Bosco A, Bratina A, et al. Epstein-Barr virus is associated with grey matter atrophy in multiple sclerosis. *J Neurol Neurosurg Psychiatry.* 2009; **80**: 620–5.
28. Comabella M, Kakalacheva K, Río J, Münz C, Montalban X, Lünemann JD. EBV-specific immune responses in patients with multiple sclerosis responding to IFNβ therapy. *Mult Scler.* 2012; **18**: 605–9.
29. Park PJ. ChIP-seq: advantages and challenges of a maturing technology. *Nat Rev Genet.* 2009; **10**: 669–80.
30. Satoh J. Bioinformatics approach to identifying molecular biomarkers and networks in multiple sclerosis. *Clin Exp Neuroimmunol.* 2010; **1**: 127–40.
31. Satoh J, Tabunoki H. Molecular network of ChIP-Seq-based vitamin D receptor target genes. *Mult Scler.* 2013; **19**: 1035–45.
32. da Huang W, Sherman BT, Lempicki RA. Systematic and integrative analysis of large gene lists using DAVID bioinformatics resources. *Nat Protoc.* 2009; **4**: 44–57.
33. Zhao B, Zou J, Wang H, Johannsen E, Peng CW, Quackenbush J, et al. Epstein-Barr virus exploits intrinsic B-lymphocyte transcription programs to achieve immortal cell growth. *Proc Natl Acad Sci USA.* 2011; **108**: 14902–7.
34. Klein SC, Jücker M, Abts H, Tesch H. IL6 and IL6 receptor expression in Burkitt's lymphoma and lymphoblastoid cell lines: promotion of IL6 receptor expression by EBV. *Hematol Oncol.* 1995; **13**: 121–30.
35. Landt SG, Marinov GK, Kundaje A, Kheradpour P, Pauli F, Batzoglou S, et al. ChIP-seq guidelines and practices of the ENCODE and modENCODE consortia. *Genome Res.* 2012; **22**: 1813–31.
36. Coppotelli G, Mughal N, Callegari S, Sompallae R, Caja L, Luijsterburg MS, et al. The Epstein-Barr virus nuclear antigen-1 reprograms transcription by mimicry of high mobility group A proteins. *Nucleic Acids Res.* 2013; **41**: 2950–62.
37. Wood VH, O'Neil JD, Wei W, Stewart SE, Dawson CW, Young LS. Epstein-Barr virus-encoded EBNA1 regulates cellular gene transcription and modulates the STAT1 and TGFb signaling pathways. *Oncogene.* 2007; **26**: 4135–47.
38. Schaefer BC, Paulson E, Strominger JL, Speck SH. Constitutive activation of Epstein-Barr virus (EBV) nuclear antigen 1 gene transcription by IRF1 and IRF2 during restricted EBV latency. *Mol Cell Biol.* 1997; **17**: 873–86.
39. Bentz GL, Liu R, Hahn AM, Shackelford J, Pagano JS. Epstein-Barr virus BRLF1 inhibits transcription of IRF3 and IRF7 and suppresses induction of interferon-β. *Virology.* 2010; **402**: 121–8.
40. Wu L, Fossum E, Joo CH, Inn KS, Shin YC, Johannsen E, et al. Epstein-Barr virus LF2: an antagonist to type I interferon. *J Virol.* 2009; **83**: 1140–6.
41. Flavell JR, Baumforth KR, Wood VH, Davies GL, Wei W, Reynolds GM, et al. Down-regulation of the TGF-beta target gene, *PTPRK*, by the Epstein-Barr virus encoded

EBNA1 contributes to the growth and survival of Hodgkin lymphoma cells. *Blood.* 2008; **111**: 292–301.
42. Forte E, Luftig MA. MDM2-dependent inhibition of p53 is required for Epstein-Barr virus B-cell growth transformation and infected-cell survival. *J Virol.* 2009; **83**: 2491–9.

Supporting Information

Additional Supporting Information may be found in the online version of this article:

Figure S1 FastQC analysis of chromatin immunoprecipitation followed by deep sequencing (ChIP-Seq) data.

Table S1 The list of 92 MS-linked molecules of the KeyMolnet library.

Table S2 The list of 228 ChIP-Seq-based EBNA1-target cellular genes.

Clinical & Experimental Neuroimmunology

Clinical and Experimental Neuroimmunology **4** (2013) 296–304

ORIGINAL ARTICLE

Reactive astrocytes and perivascular macrophages express NLRP3 inflammasome in active demyelinating lesions of multiple sclerosis and necrotic lesions of neuromyelitis optica and cerebral infarction

Natsuki Kawana,[1] Yoji Yamamoto,[1] Tsuyoshi Ishida,[2] Yuko Saito,[3] Hidehiko Konno,[4] Kunimasa Arima[5] and Jun-ichi Satoh[1]

[1]Department of Bioinformatics and Molecular Neuropathology, Meiji Pharmaceutical University, Tokyo, [2]Department of Pathology and Laboratory Medicine, Kohnodai Hospital, NCGM, Chiba, [3]Department of Laboratory Medicine, National Center Hospital, NCNP, Tokyo, [4]Department of Neurology, Nishitaga National Hospital, Sendai, [5]Department of Psychiatry, National Center Hospital, NCNP, Tokyo, Japan

Keywords
ASC; caspase-1; inflammasome; multiple sclerosis; NLRP3; perivascular macrophages; reactive astrocytes

Correspondence
Jun-ichi Satoh, Department of Bioinformatics and Molecular Neuropathology, Meiji Pharmaceutical University, 2-522-1 Noshio, Kiyose, Tokyo 204-8588, Japan.
Tel/Fax: +81-42-495-8678
Email: satoj@my-pharm.ac.jp

Received: 10 August 2013; revised: 18 September 2013; accepted: 25 September 2013.

Abstract

Objective Inflammasome, activated by pathogen-derived and host-derived danger signals, constitutes a multimolecular signaling complex that serves as a platform for caspase-1 (CASP1) activation and interleukin-1β (IL-1B) maturation. Mice deficient for NLRP3 inflammasome components are resistant to experimental autoimmune encephalomyelitis (EAE), suggesting a pro-inflammatory role of NLRP3 inflammasome. However, at present, a pathological role of NLRP3 inflammasome in multiple sclerosis (MS) brains remains unknown.

Methods We studied the expression of NLRP3 inflammasome components in active demyelinating lesions of MS by immunohistochemistry.

Results Reactive astrocytes and perivascular macrophages expressed all three components of NLRP3 inflammasome – NLRP3, ASC and CASP1 – along with IL-1B in active demyelinating lesions of MS, active necrotic lesions of neuromyelitis optica (NMO) and acute necrotic lesions of cerebral infarction. In contrast, the levels of expression of NLRP3, ASC, CASP1, and IL-1B were greatly reduced in chronic inactive lesions of MS and gliotic lesions of cerebral infarction. Furthermore, the great majority of ramified and amoeboid microglia did not express NLRP3 in active and inactive MS lesions.

Conclusions NLRP3 inflammasome could be activated chiefly in reactive astrocytes and infiltrating macrophages under the condition of active destruction of brain tissues that potentially provides a danger signal. (doi: 10.1111/cen3.12068, October 2013)

Introduction

Inflammasome constitutes an intracellular multimolecular signaling complex that serves as a platform for caspase-1 (CASP1) activation, interleukin-1β (IL-1B) maturation and execution of pyroptosis, a lytic form of cell death with combined characteristics of both apoptosis and necrosis.[1,2] Inflammasome formation is induced by various inflammation-inducing stimuli recognized by a cytosolic sensor called the NOD-like receptors (NLR). Inflammasome-activating signals include both microbe-derived pathogen-associated molecular patterns (PAMP) and host- or environment-derived danger-associated molecular patterns (DAMP), indicating that inflammasome acts as a master regulator of inflammation against infection and stressful insults.[1,2] Inflammasome is constructed in the cellular cytoplasm by ordered assembly of self-oligomerizing components and degraded by autophagy after ubiquitination.[3]

Among various classes of inflammasome, the nucleotide-binding oligomerization domain, leucine rich repeat and pyrin domain containing 3 (NLRP3) inflammasome represents the most extensively

characterized inflammasome. It is composed of NLRP3, the adaptor molecule named apoptosis-associated speck-like protein containing a caspase recruitment domain (ASC) and CASP1.[1,2] NLRP3 contains a central nucleotide-binding and oligomerization (NACHT) domain essential for activation of the signaling complex through adenosine 5′-triphosphate (ATP)-dependent oligomerization, flanked by a C-terminal leucine-rich repeat (LRR) pivotal for ligand sensing and autoregulation, and a N-terminal pyrin (PYD) domain involved in a homotypic protein–protein interaction between NLRP3 and ASC. The molecular interaction of NLRP3 with ASC recruits procaspase-1 by a homotypic interaction of caspase activation and recruitment (CARD) domains between ASC and procaspase-1. Subsequently, the proximity-induced procaspase-1 oligomerization causes autocatalytic activation of CASP1, followed by processing of pro-IL-1B or pro-IL-18 into biologically active IL-1B and IL-18. These cytokines act as a central regulator for induction of pro-inflammatory cytokines and chemokines that amplify inflammation by recruiting immune effector cells.

The activation of NLRP3 inflammasome is tightly regulated by two-step signals.[4] The first priming signal, such as lipopolysaccharide (LPS), enhances the expression of inflammasome components and target proteins through activation of transcription factor NF-κB. The second activation signal promotes the assembly of inflammasome components. The second signal involves three major mechanisms, including generation of reactive oxygen species (ROS), lysosomal damage and the potassium efflux.[1,2] Mitochondria serve as the principal source of ROS. Blockade of mitophagy induces accumulation of ROS-generating mitochondria that activates NLRP3 inflammasome.[5] Oxidized mitochondrial DNA directly activates NLRP3 inflammasome after induction of apoptosis.[6]

A diverse range of danger signals having DAMP, such as amyloid-β (Aβ), α-synuclein, prion fibrils, uric acid, cholesterol crystals, asbestos, silica, alum, hyaluronan and ATP, and those with PAMP, such as *Listeria monocytogenes*, *Candida albicans* and influenza A virus, effectively activate the NLRP3 inflammasome.[1,2,7–10] The pattern-recognition receptor, CD36, plays a key role in activation of NLRP3 inflammasome by priming transcription of IL-1B and facilitating the assembly of the NLRP3 inflammasome complex.[11]

Deregulated activation of NLRP3 inflammasome contributes to the pathological processes of gout, atherosclerosis, type 2 diabetes, Crohn's disease, viral encephalitis, bacterial meningitis, traumatic brain injury and Alzheimer's disease (AD).[1,2,12–15] A lack of NLRP3 inflammasome components skews microglial cells to an anti-inflammatory M2 phenotype with an enhanced capacity of Aβ clearance in a mouse model of AD.[15] Furthermore, several gain-of-function mutations in the *NLRP3* gene cause a panel of dominantly inherited diseases named cryopyrin-associated period syndromes (CAPS), composed of Muckle–Wells syndrome (MWS), familial cold autoinflammatory syndrome (FACS) and chronic infantile cutaneous neurological articular syndrome (CINCA).[1,2] They are characterized by skin rashes, episodic fever, multiple sclerosis (MS)-like inflammatory demyelinating lesions in the brain and effectiveness of anti-IL-1B therapy.[16,17]

At present, a pathological role of NLRP3 inflammasome in MS brains remains largely unknown. A previous study showed that CASP1 is expressed in both macrophages/microglia and oligodendrocytes in acute and chronic MS lesions.[18] In a cuprizone-induced demyelination model of MS, mice lacking the *NLRP3* gene showed delayed neuroinflammation and demyelination, indicating that NLRP3 exacerbates inflammatory demyelination in the central nervous system (CNS).[19] NLRP3 expression levels were elevated in the spinal cord during myelin oligodendrocyte glycoprotein (MOG)-induced experimental autoimmune encephalomyelitis (EAE), a mouse model of MS; and on induction of EAE, *NLRP3*-knockout mice showed a delayed clinical course and reduced severity of the disease, accompanied by substantial attenuation of inflammation, demyelination and astrogliosis.[20] Furthermore, mice deficient for ASC or CASP1 are also resistant to EAE, suggesting a pro-inflammatory role of NLRP3 inflammasome.[21] Interferon-β (IFNβ) inhibits NLRP3 inflammasome activation by inducing undefined molecules through STAT1 signaling.[22] Monocytes derived from IFNβ-treated MS patients showed decreased IL-1B production in response to inflammasome-activating stimuli.[22] All of these observations suggest that NLRP3 inflammasome might play a crucial role in the immunopathogenesis of MS.

The present study for the first time attempts to characterize the expression of NLRP3 inflammasome components in active demyelinating lesions of MS by immunohistochemistry.

Methods

Human brain tissues

For immunohistochemistry, 10 micron-thick serial sections of the cerebral cortex were prepared from

autopsied brains of four MS patients and nine non-MS subjects. All four MS cases were clinically diagnosed as chronic progressive MS, composed of three cases of secondary progressive MS (SPMS) and one case of primary progressive MS (PPMS). Non-MS cases included a previously reported case of neuromyelitis optica (NMO),[23] four neurologically normal control (NC) subjects and four patients with cerebral infarction. Their clinical characteristics are shown in Table S1. Autopsies were carried out at the National Center Hospital, National Center of Neurology and Psychiatry (NCNP), Kohnodai Hospital, National Center for Global Health and Medicine (NCGM) or the Nishitaga National Hospital. The comprehensive examination by three established neuropathologists (KA, YS, TI) validated the pathological diagnosis. Written informed consent was obtained from all the cases. The ethics committee of the corresponding institutions approved the present study.

Immunohistochemistry

Immunohistochemical studies were carried out according to the methods described previously.[24] In brief, after deparaffination, tissue sections were heated in 10 mM citrate sodium buffer, pH 6.0 by autoclave at 110°C for 15 min in a temperature-controlled pressure chamber (Biocare Medical, Concord, CA, USA). They were treated at room temperature for 15 min with 3% hydrogen peroxide-containing methanol to block the endogenous peroxidase activity. The tissue sections were then incubated with phosphate-buffered saline (PBS) containing 10% normal goat serum at room temperature for 15 min to block non-specific staining. They were incubated in a moist chamber at 4°C overnight with a rabbit antibody against the peptide mapping to the N-terminus of the human NLRP3 protein (1:300; HPA012878; Sigma, St. Louis, MO, USA), a rabbit antibody against a mixture of the peptides mapping at amino acid residues 31–46 and 94–110 of the human ASC protein (1:100; ab113225; Abcam, Cambridge, England), a rabbit antibody against the C-terminal peptide of the human CASP1 p10 protein (1:500; sc-515; Santa Cruz Biotechnology, Santa Cruz, CA, USA) and a rabbit antibody against the peptide mapping at amino acid residues of 117–269 of the human IL-1B protein (1:50; sc-7884; Santa Cruz Biotechnology). After washing with PBS, the tissue sections were labeled at room temperature for 30 min with horseradish peroxidase (HRP)-conjugated secondary antibodies (Nichirei, Tokyo, Japan), followed by incubation with diaminobenzidine tetrahydrochloride (DAB) substrate (Vector, Burlingame, CA, USA). They were processed for a counterstain with hematoxylin. Negative controls underwent all the steps except for exposure to primary antibody. We classified chronic demyelinating lesions of MS into either "chronic active", defined as a lesion with a hypocellular center and a hypercellular rim, or "chronic inactive", defined as a hypocellular lesion.[25]

For double labeling, tissue sections were initially stained with anti-NLRP3 antibody HPA012878. After autoclaving, they were labeled with prediluted mouse antibodies against GFAP (GA5; Nichirei) or CD68 (KP1; Dako, Tokyo, Japan), followed by incubation with alkaline phosphatase (AP)-conjugated secondary antibodies (Nichirei) and colorized with a Warp Red chromogen (Biocare Medical, Concord, CA, USA).

Reverse transcription polymerase chain reaction analysis

Total RNA was isolated from a panel of human cell lines described previously.[26] Total RNA of the human frontal cerebral cortex (Clontech, Mountain View, CA, USA) was also processed in parallel for reverse transcription polymerase chain reaction (RT–PCR). DNase-treated total RNA was processed for cDNA synthesis using oligo(dT)$_{12-18}$ primers and SuperScript II reverse transcriptase (Invitrogen, Carlsbad, CA, USA). Then, cDNA was amplified by PCR using HotStar Taq DNA polymerase (Qiagen, Valencia, CA, USA), and the following panel of sense and antisense primer sets: 5′ agtgctgaaacagcagagctgcct3′ and 5′ccgtttccactcctaccaagaagg3′ for a 151 bp product of *NLRP3*; 5′ agtttcacaccagcctggaactgg3′ and 5′ggatgatttggtgggattgccagg3′ for a 153 bp product of *ASC*; 5′tggagacatcccacaatgggctct3′ and 5′cactctttcagtggtgggcatctg3′ for an 159 bp product of *CASP1*; 5′tgcccagttccccaactggtacat3′ and 5′ aggactctctgggtacagctctct3′ for a 145 bp product of *IL-1B*; and 5′ccatgttcgtcatgggtgtgaacca3′ and 5′gccagtagaggcagggatgatgttc3′ for a 251 bp product of the *glyceraldehyde-3-phosphate dehydrogenase* (*G3PDH*) gene that serves as an internal control. The amplification program consisted of an initial denaturing step at 95°C for 15 min, followed by a denaturing step at 94°C for 1 min, an annealing step at 60°C for 40 s and an extension step at 72.9°C for 50 s for 35 cycles, except for G3PDH amplified for 28 cycles.

Transient expression of NLRP3, ASC, and CASP1 in HEK293 cells

Open reading frames (ORF) of the human *NLRP3* gene (GenBank NM_004895), the human *ASC* gene (GenBank NM_013258) and the human *CASP1* gene (GenBank NM_033292) were amplified by PCR using PfuTurbo DNA polymerase (Stratagene, La Jolla, CA, USA), and the following sense and antisense primer sets: 5'gcaagcacccgctgcaagctggcc3' and 5'ctaccaagaaggctcaaagacgac3' for *NLRP3*, 5' gggcgcg cgcgcgacgccatcctg3' and 5'tcagctccgctccaggtcctccac3' for *ASC*, and 5' gccgacaaggtcctgaaggagaag3' and 5' ttaatgtcctgggaagaggtagaa3' for *CASP1*. Then, they were cloned in a mammalian expression vector named pcDNA4/HisMax-TOPO (Invitrogen). Then, the vectors were transfected into HEK293 cells by using Lipofectamine 2000 reagent (Invitrogen). At 24 h after transfection, the cells were processed for western blot analysis.

Western blot analysis

To prepare the total protein extract, the cells were homogenized in RIPA lysis buffer (Sigma) and a cocktail of protease inhibitors, followed by centrifugation at 13 400 rpm for 5 min at room temperature. The supernatant was separated on a 12% sodium dodecylsulfate polyacrylamide gel electrophoresis gel. After gel electrophoresis, the protein was transferred onto nitrocellulose membranes, and immunolabeled at room temperature overnight with the aforementioned primary antibodies. Then, the membranes were incubated at room temperature for 30 min with HRP-conjugated secondary antibodies (Santa Cruz Biotechnology). The specific reaction was visualized by using a chemiluminescent substrate (Pierce, Rockford, IL, USA). After the antibodies were stripped by incubating the membranes at 50°C for 30 min in a stripping buffer composed of 62.5 mM Tris-HCl, pH 6.7, 2% sodium dodecylsulfate and 100 mM 2-mercaptoethanol, the membranes were relabeled with a goat anti-heat shock protein HSP60 antibody (sc-1052; Santa Cruz Biotechnology) to assess an internal control for protein loading.

Results

Expression of NLRP3 inflammasome components in human neural cell lines

First, we studied NLRP3, ASC, CASP1 and IL-1B mRNA expression in a panel of human neural cell lines by RT–PCR. The complete set of NLRP3, ASC, CASP1 and IL-1B mRNA were expressed at variable levels in human cerebral (CBR) brain tissues, astrocytes (AS), neural progenitor (NP) cells, NTera2-deived differentiated neurons (NTera2N), T98G glioblastoma and HMO6 microglia, where the levels of G3PDH, a housekeeping gene, were almost constant (Fig. 1a–e; lanes 1, 3–5, 9, 10). When omitting the RT step, no PCR products were amplified (Fig. 1a–e; lane 2). The highest levels of NLRP3 and IL-1B were identified in NTera2N, whereas the highest levels of ASC and CASP1 were found in T98G. These results showed that the levels of the constitutive expression of NLRP3 inflammasome components are highly variable among distinct neural cell types.

Expression of NLRP3 inflammasome components in reactive astrocytes and perivascular macrophages in chronic active demyelinating lesions of MS, active necrotic lesions of NMO, and acute infarct lesions

Next, to verify the specificity of anti-NLRP3 antibody (HPA012878), anti-ASC antibody (ab113225) and

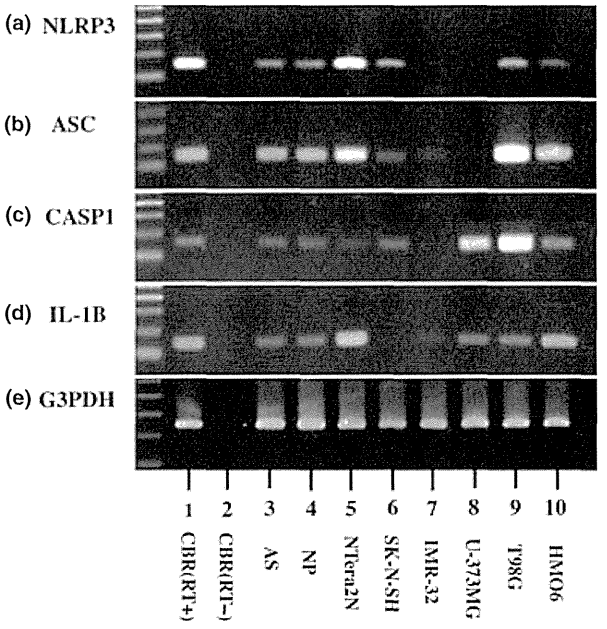

Figure 1 The expression of NLRP3 inflammasome components in human neural cell lines. The mRNA expression of (a) NLRP3, (b) ASC, (c) caspase-1 (CASP1), and (d) interleukin (IL)-1B, and (e) glyceraldehyde-3-phosphate dehydrogenase (G3PDH) was studied by reverse transcription (RT) polymerase chain reaction in human brain tissues and neural cell lines in culture. The lanes represent (1) cerebral (CBR) brain tissues with inclusion of RT step, (2) CBR without inclusion of RT-step, (3) astrocytes (AS), (4) neural progenitor (NP) cells, (5) NTera2-deived differentiated neurons (NTera2N), (6) SK-N-SH neuroblastoma, (7) IMR-32 neuroblastoma, (8) U-373MG astrocytoma, (9) T98G glioblastoma and (10) HMO6 microglia.

anti-CASP1 antibody (sc-515) utilized in the present study, the human *NLRP3*, *ASC* and *CASP1* genes cloned in the mammalian expression vector were expressed in HEK293 cells for western blot analysis. HPA012878, ab113225 and sc-515 reacted individually with the corresponding recombinant proteins of NLRP3, ASC or CASP1, but not with protein extract isolated from non-transfected cells (Fig. S1a–c). These results validated the specificity of the antibodies tested.

Then, we studied the expression of three components of NLRP3 inflammasome, along with IL-1B, in the cerebral cortex sections of four MS and nine non-MS cases by immunohistochemistry using the aforementioned antibodies. In the brains of neurologically normal control (NC) subjects, NLRP3 expression was restricted in a rare population (less than 0.01% of total cells) that represent a specified subset of ramified microglial cells often located in deep cortical layers and the white matter (Fig. S2a). All neurons, oligodendrocytes, astrocytes and the great majority of ramified microglia did not express discernible levels of NLRP3. In NC brains, ASC and CASP1 were undetectable except for a small subset (less than 0.1%) of ramified microglia (Fig. S2b,c). In contrast, IL-1B was expressed in many neurons with the location in the cytoplasm and in a small population (less than 1%) of ramified microglia (Fig. S2d).

Notably, numerous reactive astrocytes accumulating in chronic active demyelinating lesions of MS expressed intense immunoreactivities for NLRP3, ASC, CASP and IL-1B with the location in the cytoplasm (Fig. 2a–d, Fig. 3e). In contrast, the levels of expression of NLRP3, ASC, CASP, and IL-1B were much lower in reactive astrocytes and glial scars in chronic inactive lesions of MS. Furthermore, a large number of perivascular foamy macrophages expressed NLRP3, ASC, CASP and IL-1B at variable intensities in chronic active demyelinating lesions of MS (Fig. 3a–d,f). In contrast, the great majority of amoeboid and ramified microglia did not express NLRP3 in chronic active and inactive MS lesions (Fig. 3g). In the edge of active necrotic lesions of NMO, only hypertrophic reactive astrocytes and foamy macrophages intensely expressed the full set of NLRP3, ASC, CASP, and IL-1B (Fig. 4a–d). These results showed that reactive astrocytes and infiltrating macrophages engulfing tissue debris are the major cell types that express the complete set of NLRP3 components in active MS and NMO lesions.

In acute lesions of cerebral infarction, reactive astrocytes surrounding ischemic cores and foamy macrophages accumulating in necrotic lesions moderately expressed NLRP3, ASC, CASP, and IL-1B (Fig. 5a–d). In contrast, the levels of expression of NLRP3, ASC, CASP and IL-1B were low in any cell types in chronic gliotic lesions of cerebral infarction.

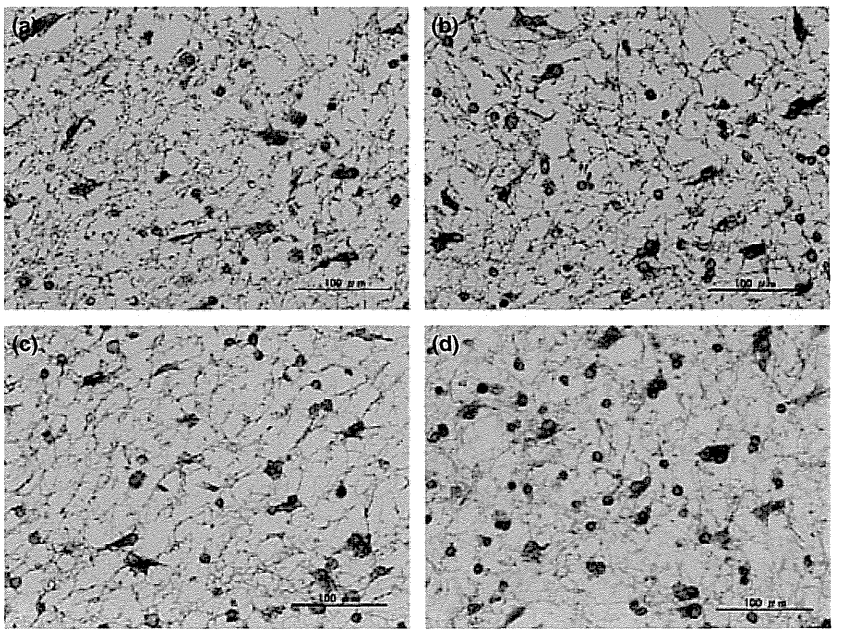

Figure 2 The expression of NLRP3 inflammasome components in reactive astrocytes in chronic active demyelinating lesions of multiple sclerosis. The expression of (a) NLRP3, (b) ASC, (c) caspase-1 and (d) interleukin-1B was studied in the serial sections of chronic active lesions of multiple sclerosis by immunohistochemistry. Reactive astrocytes intensely expressed all three components and interleukin -1B with the location of the cytoplasm.

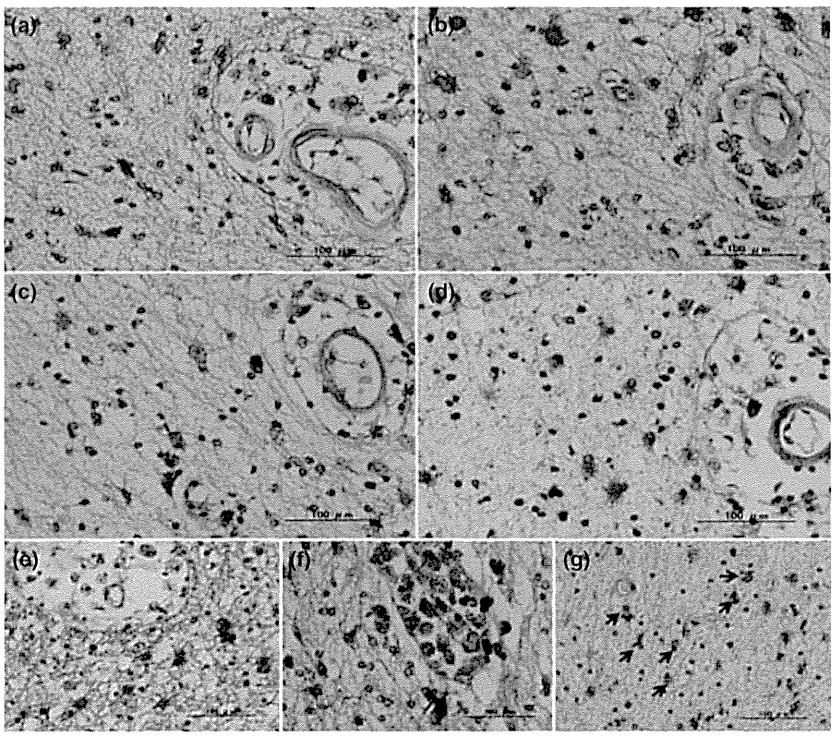

Figure 3 The expression of NLRP3 inflammasome components in perivascular macrophages in chronic active demyelinating lesions of multiple sclerosis. The expression of (a) NLRP3, (b) ASC, (c) caspase-1 and (d) interleukin-1B was studied in the serial sections of chronic active lesions of multiple sclerosis by immunohistochemistry. Perivascular macrophages expressed variable intensities of all three components and interleukin-1B in the cytoplasm. (e–g) Double immunolabeling of (e) NLRP3 (brown) and GFAP (red), (f) NLRP3 (brown) and CD68 (red), and (g) NLRP3 (brown) and CD68 (red). The arrows indicate CD68-positive NLRP3-negative ameboid microglial cells.

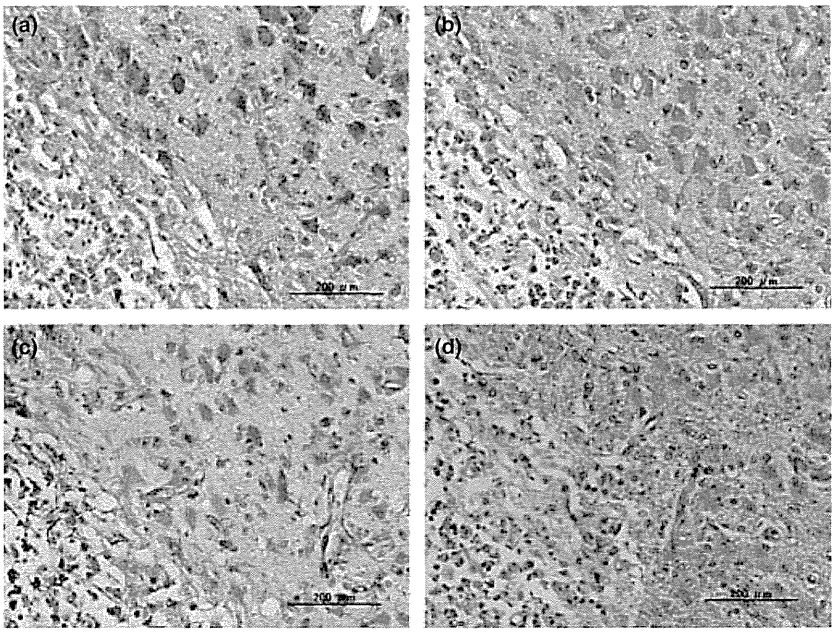

Figure 4 The expression of NLRP3 inflammasome components in reactive hypertrophic astrocytes and infiltrating macrophages in active necrotic lesions of neuromyelitis optica (NMO). The expression of (a) NLRP3, (b) ASC, (c) caspase-1 and (d) interleukin-1B was studied in the serial sections of active necrotic lesions of NMO by immunohistochemistry. Hypertrophic reactive astrocytes in the right upper half and foamy macrophages in the left lower half intensely expressed all three components and interleukin-1B with the location in the cytoplasm.

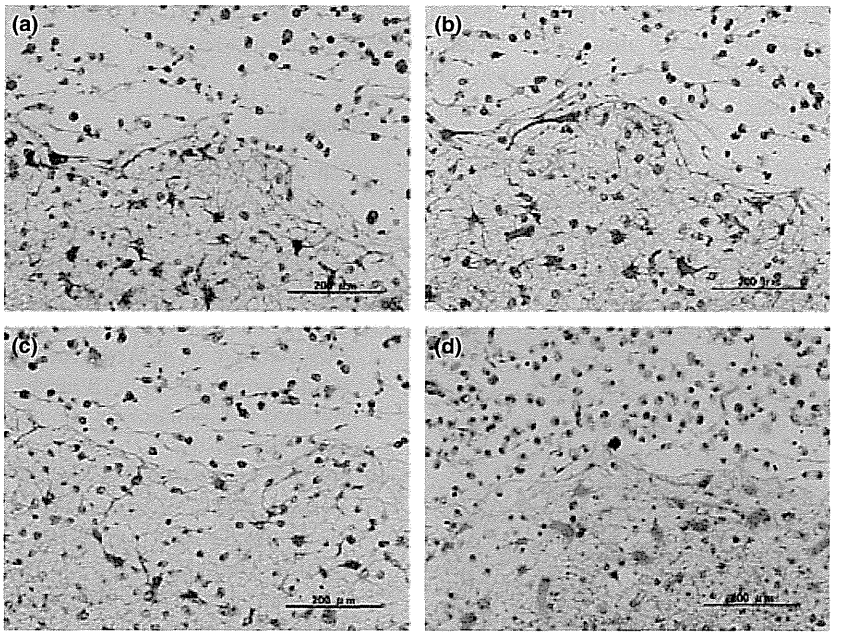

Figure 5 The expression of NLRP3 inflammasome components in reactive astrocytes and infiltrating macrophages in acute necrotic lesions of cerebral infarction. The expression of (a) NLRP3, (b) ASC, (c) caspase-1 and (d) interleukin-1B was studied in the serial sections of acute necrotic lesions of cerebral infarction by immunohistochemistry. Reactive astrocytes and foamy macrophages moderately expressed all three components and interleukin -1B with the location in the cytoplasm.

These results showed that NLRP3 inflammasome could be activated chiefly in astrocytes and macrophages under the condition of active destruction of brain tissues, regardless of the etiology, such as MS, NMO and cerebral infarction.

Discussion

By immunohistochemistry, we showed that reactive astrocytes and infiltrating foamy macrophages express the complete set of NLRP3 inflammasome components, such as NLRP3, ASC and CASP1, along with IL-1B in active demyelinating lesions of MS, active necrotic lesions of NMO and acute necrotic lesions of cerebral infarction. In contrast, the levels of expression of NLRP3, ASC, CASP, and IL-1B were substantially reduced in chronic inactive lesions of MS and chronic gliotic lesions of cerebral infarction, when compared with the expression levels in active demyelinating and necrotic lesions. We also found that the great majority of ramified and amoeboid microglia did not express NLRP3 in active and inactive MS lesions, and active NMO and infarct lesions. These results apparently contradict the observations of NLRP3 expression in HMO6 human microglial cells by RT–PCR, and the microglial expression of NLRP3 in a mouse model of AD.[15] However, a recent study elucidated NLRP3 inflammasome-independent mechanisms of IL-1B and IL-18 maturation in microglia.[27] Our observations suggest that NLRP3 inflammasome could be activated chiefly in astrocytes and macrophages under the condition of active destruction of brain tissues that potentially provides a danger signal, regardless of the etiology, such as MS, NMO and cerebral infarction. However, in the present study, the main limitation exists in non-quantitative analysis as a result of a small sample size analyzed by immunohistochemistry. To overcome this drawback, further examinations on large cohorts, including frozen brain tissues by western blot analysis, would be required.

Accumulating evidence shows that a diverse range of danger signals containing DAMP and PAMP effectively activate NLRP3 inflammasome.[1,2,7–10] Among the host-derived signals with DAMP, ATP is released extracellularly from damaged or dying cells after injury, infection and inflammation.[7,12] The activation of NLRP3 inflammasome in response to extracellular ATP is mediated by the purinergic receptor, P2X7, which recruits the pannexin-1 membrane channel.[7] Importantly, EAE is ameliorated by P2X7 receptor blockade.[28] Furthermore, the levels of P2X7 receptor expression are elevated in activated macrophages/microglia in the spinal cord of MS, suggesting the possible contribution of extracellular ATP to activation of NLRP3 in MS lesions.[29] Astrocytes also

express a P2X7 receptor and respond well to extracellular ATP.[30] It is worthy to note that acidic extracellular pH as a result of active destruction of brain tissues promotes NLRP3 inflammasome activation.[31]

A recent study showed that nanoparticles, such as 20 nm latex beads, could activate NLRP3 inflammasome in bone marrow-derived macrophages.[32] We could raise a possible scenario that brain tissue debris containing myelin degradation products of nanoparticle size, when taken up by phagocytosis, might serve as a danger signal for activation of NLRP3 inflammasome in infiltrating macrophages in active MS, NMO and infarct lesions. Furthermore, reactive astrocytes, as well as professional phagocytes, such as macrophages, microglia and dendritic cells, have a capacity to phagocytose damaged cells.[33] Mitochondrial injury generates excessive amounts of ROS in active MS lesions,[34] which potentially accelerates the assembly of NLRP3 inflammasome complex. NLRP3, translocated to mitochondria after activation of the inflammasome, regulates mitochondrial homeostasis.[35] Importantly, IFNβ inhibits activation of Rac1 through the SOCS1 signaling pathway, and reduces the generation of ROS.[36] Treatment with IFNβ is highly effective in a subtype of EAE whose development depends primarily on NLRP3 inflammasome, whereas it is ineffective in a distinct subtype of EAE independent of NLRP3 inflammasome activation induced by aggressive immunization.[36] In EAE, NLRP3 inflammasome promotes chemotactic migration of CD4+ T cells and antigen-presenting cells into the CNS, supporting a pro-inflammatory role of NLRP3 inflammasome.[37]

As clearance of damaged cellular constituents by locally accumulated phagocytes is a fundamental process to limit tissue damage, the present observations suggest the hypothesis that NLRP3 inflammasome expressed in reactive astrocytes and infiltrating macrophages plays a key role in not only amplification of inflammation, but also facilitation of tissue repair and regeneration by rapid and efficient production of IL-1B, serving as a potent growth factor for neural precursor cells, in MS, NMO and infarct lesions after acute tissue destruction.[38]

Acknowledgements

All autopsied brain samples were provided by Research Resource Network (RRN), Japan. This work was supported by grants from the JSPS KAKENHI (C22500322 and C25430054), the Ministry of Education, Culture, Sports, Science and Technology (MEXT), Japan. The authors declare no conflict of interest.

References

1. Schroder K, Tschopp J. The inflammasomes. *Cell*. 2010; **140**: 821–32.
2. Menu P, Vince JE. The NLRP3 inflammasome in health and disease: the good, the bad and the ugly. *Clin Exp Immunol*. 2011; **166**: 1–15.
3. Shi CS, Shenderov K, Huang NN, Kabat J, Abu-Asab M, Fitzgerald KA, et al. Activation of autophagy by inflammatory signals limits IL-1β production by targeting ubiquitinated inflammasomes for destruction. *Nat Immunol*. 2012; **13**: 255–63.
4. Wang H, Mao L, Meng G. The NLRP3 inflammasome activation in human or mouse cells, sensitivity causes puzzle. *Protein Cell*. 2013; **4**: 565–8.
5. Zhou R, Yazdi AS, Menu P, Tschopp J. A role for mitochondria in NLRP3 inflammasome activation. *Nature*. 2011; **469**: 221–5.
6. Shimada K, Crother TR, Karlin J, Dagvadorj J, Chiba N, Chen S, et al. Oxidized mitochondrial DNA activates the NLRP3 inflammasome during apoptosis. *Immunity*. 2012; **36**: 401–14.
7. Di Virgilio F. Liaisons dangereuses: $P2X_7$ and the inflammasome. *Trends Pharmacol Sci*. 2007; **28**: 465–72.
8. Halle A, Hornung V, Petzold GC, Stewart CR, Monks BG, Reinheckel T, et al. The NALP3 inflammasome is involved in the innate immune response to amyloid-β. *Nat Immunol*. 2008; **9**: 857–65.
9. Hafner-Bratkovič I, Benčina M, Fitzgerald KA, Golenbock D, Jerala R. NLRP3 inflammasome activation in macrophage cell lines by prion protein fibrils as the source of IL-1β and neuronal toxicity. *Cell Mol Life Sci*. 2012; **69**: 4215–28.
10. Codolo G, Plotegher N, Pozzobon T, Brucale M, Tessari I, Bubacco L, et al. Triggering of inflammasome by aggregated α-synuclein, an inflammatory response in synucleinopathies. *PLoS ONE*. 2013; **8**: e55375.
11. Sheedy FJ, Grebe A, Rayner KJ, Kalantari P, Ramkhelawon B, Carpenter SB, et al. CD36 coordinates NLRP3 inflammasome activation by facilitating intracellular nucleation of soluble ligands into particulate ligands in sterile inflammation. *Nat Immunol*. 2013; **14**: 812–20.
12. Hoegen T, Tremel N, Klein M, Angele B, Wagner H, Kirschning C, et al. The NLRP3 inflammasome contributes to brain injury in pneumococcal meningitis and is activated through ATP-dependent lysosomal cathepsin B release. *J Immunol*. 2011; **187**: 5440–51.
13. Kaushik DK, Gupta M, Kumawat KL, Basu A. NLRP3 inflammasome: key mediator of neuroinflammation in murine Japanese encephalitis. *PLoS ONE*. 2012; **7**: e32270.

